

## FEMTOSLICING IN STORAGE RINGS \*

S. Khan, BESSY, 12489 Berlin, Germany

### Abstract

The generation of ultrashort synchrotron radiation pulses by laser-induced energy modulation of electrons and their subsequent transverse displacement ("femtosing") was demonstrated at the Advanced Light Source in Berkeley. More recently, a femtoslicing facility was commissioned at BESSY II in Berlin, and another project is in progress at the Swiss Light Source. The paper reviews the principle of femtoslicing and its technical implementations.

### INTRODUCTION

At contemporary synchrotron radiation (SR) sources, powerful x-ray techniques [1, 2] are restricted to a time resolution given by the electron bunch length of 40-100 ps (fwhm), whereas the 100-fs time scale, on which chemical reactions, phase transitions and other interatomic phenomena take place, has been accessible with optical laser pulses since the mid-1980s [3]. Apart from the development of faster detection techniques (particularly streak cameras, e.g. [4]), there are several approaches to achieve short pulse duration *and* short wavelength:

**i) converting fs laser pulses to higher photon energy** by higher-harmonic generation (HHG) [5], by creating a plasma that emits x-rays [6], or by relativistic Thomson scattering [7];

**ii) changing the time structure of electron bunches** by reducing the momentum-compaction factor in a storage ring [8], by laser-induced energy modulation ("femtosing") [9], by orbit deflection with crab cavities [10], or by bunch compression in linear accelerators, particularly in combination with a free-electron laser (FEL) [11, 12].

In the second category, only laser-based techniques (femtosing and seeded FELs) provide natural synchronization between laser pulses and x-rays for pump-probe applications.

Femtosing was proposed in 1996 by A. Zholents and M. Zoloterev [9] as a technique to generate ultrashort x-ray pulses at SR facilities, and was experimentally demonstrated at the Advanced Light Source (ALS) in Berkeley [13]. In 2004, the first undulator-baser femtoslicing source was completed at BESSY II in Berlin [14], and a third facility at the Swiss Light Source (SLS) is scheduled for the end of 2005 [15]. Femtoslicing adds a new quality to existing SR facilities and allows to gain hands-on experience with laser-induced energy modulation, which is the basis of various schemes for FEL seeding [16, 17] and attosecond-pulse generation [18, 19, 20] at future facilities.

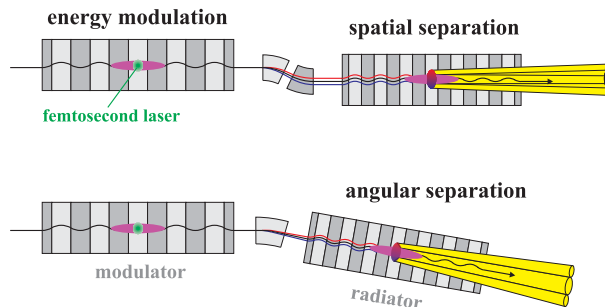


Figure 1: Generation of short x-ray pulses by laser-induced energy modulation of electrons and subsequent spatial (top) and angular (bottom) separation.

### THE PRINCIPLE OF FEMTOSLICING

Figure 1 sketches two variations of the femtoslicing principle, where a femtosecond laser pulse copropagates with an electron bunch in an undulator (the "modulator") and modulates the electron energy. Subsequent magnets translate the energy modulation into a parallel (top) or angular displacement (bottom) of electrons – or a combination of both – to separate long and short-pulse radiation emitted by the "radiator", which may be a bend magnet or any type of insertion device.

### Separation Schemes

Several separation methods have been proposed [21]: If the angular displacement exceeds the opening angle of the radiation, the short-pulse component can be separated just by an aperture. Otherwise, an aperture is placed in the image plane of the beamline optics. However, non-specular scattering due to the surface roughness of mirrors may cause excessive background. Additional background may come from non-Gaussian beam tails [22], whereas in angular separation the radiation angle dominates over the electron divergence and beam tails are negligible. For an undulator with extremely small bandwidth, the energy shift of radiation from off-energy electrons may also be used to separate it from the long pulse [23]. In an angular separation scheme, even further background suppression can be achieved by additional spatial and spectral separation in the beamline. In either case, off-energy electrons may be displaced horizontally or vertically. For spatial separation, the usually much smaller vertical beam emittance suggests a vertical displacement. Angular separation involves a large bend angle between modulator and radiator, which is more practical in the horizontal plane. Application of this scheme to large-angle wiggler radiation would require the wiggler plane to be vertical.

\* Funded by the Bundesministerium für Bildung und Forschung and by the Land Berlin. Contact: shaukat.khan@bessy.de

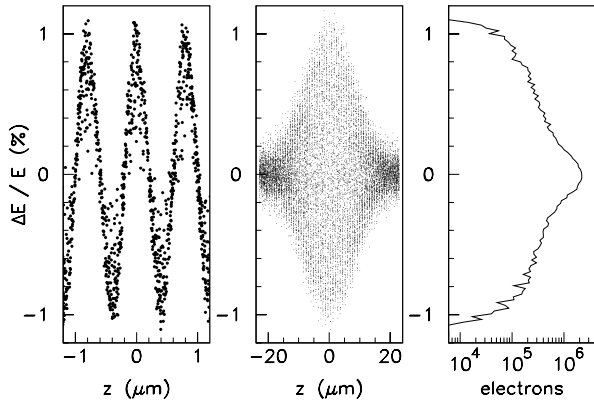


Figure 2: Simulation of laser-induced energy modulation. Left and center – electron distribution in the longitudinal phase space. Right – projection of the electron distribution over a length of 50  $\mu\text{m}$  onto the energy axis.

### Laser-Induced Energy Modulation

The energy modulation process does not produce two distinct off-energy "satellites", but a continuous distribution as shown in Fig. 2, where the interaction between 1.7 GeV electrons and a 1.5 mJ laser pulse of 45 fs duration (fwhm) was simulated. In this example, the modulation amplitude, i.e. the maximum energy deviation, is 1.1%. Energy gain and loss are equal if the modulator wavelength is slightly detuned (because of the Guoy phase shift [24]) below the value given by the resonance condition

$$\lambda_L = \frac{\lambda_U}{2\gamma^2} \left( 1 + \frac{K^2}{2} \right), \quad (1)$$

where  $\lambda_L$  is the laser wavelength,  $\gamma$  is the Lorentz factor of the electrons,  $\lambda_U$  is the modulator period length and  $K$  is its deflection parameter. The envelope of the longitudinal distribution reflects the bunch length enlarged by  $N_U \lambda_L$ , the distance by which the electrons slip relative to the laser field over  $N_U$  undulator periods. A close-up view (left part of Fig. 2) shows that the modulation oscillates with a periodicity of  $\lambda_L = 800$  nm and has low-energy tails from off-axis electrons that experience a lower laser field. The modulation amplitude is approximately given by [9]

$$\Delta E = 2 \sqrt{\pi \alpha A_L E_L \frac{K^2/2}{1 + K^2/2} \frac{N_U}{N_L}} \quad (2)$$

with the same symbols as before and  $\alpha$  being the fine structure constant,  $A_L$  being the laser pulse energy, and  $E_L$  being the photon energy. The ratio of  $N_U$  and the number of optical cycles  $N_L$  is limited to unity, since there is no further gain once the electrons slip over more than  $N_L$  wavelengths. For the case shown in Fig. 2 with  $N_U = 10$ , this equation yields an amplitude of 1.6%. Additional corrections given in [21] lead to 1.2%, which is very close to the simulation result obtained by integrating the product of

the electric laser field  $\mathcal{E}$  and the transverse electron velocity  $x' \equiv dx/ds$  over the length  $L$  of the modulator for an ensemble of randomly generated "macroelectrons":

$$\Delta E = -e \int_{-L/2}^{L/2} x'(s) \mathcal{E}(x, y, z) ds. \quad (3)$$

Both, the ALS [21] and BESSY [25] have reported the experimentally obtained energy modulation to be below the theoretical expectation, which may be due to imperfect laser-electron overlap, losses in the laser beamline, optical aberrations, mechanical vibrations or temporal jitter.

### Photon Flux and Pulse Duration

Compared to conventional SR, the femtoslicing photon flux is diluted by the ratio of laser pulse and bunch length ( $\sim 10^{-3}$ ), the ratio of laser repetition rate and bunch rate ( $\sim 10^{-5}$ ) and by the fraction of energy-modulated electrons whose radiation can be extracted ( $\sim 10^{-1}$ ). Raising the current of the interacting bunch increases the photon flux less than proportional because of bunch lengthening and even less if integrated over time, because the lifetime of the bunch is reduced [26] – unless top-up injection is employed. The photon flux is proportional to the laser repetition rate  $f_L$ , provided the bunch charge is preserved, which depends on the fill pattern. The number of required bunches is  $f_L T$ , where  $T$  is the time between interactions with the same bunch. In the BESSY case, background from previous interactions was found to be tolerable for  $T = 1$  ms, implying single-bunch operation at 1 kHz [27].

The initial length of energy-modulated electron distribution is increased by path length differences between modulator and radiator, which depend in detail on the magnetic lattice. The x-ray pulse on the sample is further lengthened in the radiator by electron slippage (periods times wavelength) and in the beamline by the product of wavelength and illuminated lines of the monochromator grating. A reasonable x-ray pulse length is 100 fs (fwhm).

## EXISTING AND PLANNED FACILITIES

Table 1 summarizes order-of-magnitude parameters for existing femtoslicing facilities and those that are scheduled for the near future, while Fig. 3 shows their simplified footprints.

**Advanced Light Source:** Early proof-of-principle experiments at the ALS [13, 21] were carried out using a bend magnet radiator 3/2 arcs downstream of the modulator (beamline 6.3.1), where "arc" refers to a triple-bend achromat. A Ti:sapphire laser system delivered 0.7 mJ pulses at a rate of 1 kHz with 50 fs (fwhm) duration. In 2004, a new modulator with  $\lambda_U = 11$  cm was installed. Moving to the bend magnet beamline 5.3.1, now 1/2 arc from the modulator, a pulse duration of 143 fs (fwhm) was measured and time-resolved near-edge x-ray absorption measurements on  $\text{VO}_2$  were performed [28]. A twofold upgrade is scheduled for summer 2005 [29], installing an in-vacuum undulator (3

Table 1: Parameters of femtoslicing facilities operational by the end of 2005

	ALS	ALS upgrade	BESSY	SLS
beam energy (GeV)	1.5-1.9	1.9	1.7	2.4
photon energy (keV)	0.5-7	0.2-10	0.4-1.4	3-8
separation scheme	hor. spatial	vert. spatial	hor. angular	hor. angular
pulse length (fs, fwhm)	100	200	100	100
photons/pulse (0.1% bw)	30	$2 \cdot 10^3$	$10^3$	$10^3$
repetition rate (kHz)	1	20	1-2	1

cm period length and 5.5 mm gap) as radiator one arc from the modulator, and upgrading the laser system to 1.5 mJ at 20 kHz repetition rate. Two beamlines (for 0.2-2 keV and 2-10 keV photon energy, respectively) are under construction. Spatial separation will be employed with a vertical dispersion bump at the radiator formed by skew quadrupole magnets [30].

**BESSY:** The layout of the femtoslicing facility at BESSY II was finalized in 2002 [31]. A planar undulator with  $\lambda_U = 139$  and  $N_U = 10$  as modulator and a 30-period elliptical undulator with 56 mm period length as radiator were placed in one 5.3 m long straight section, together with three bend magnets forming a closed bump. A bend angle of 112 mrad between modulator and radiator provides angular separation. Since the radiator is not aligned with the straight section, two existing x-ray beamlines had to be relocated, and a third beamline was added. A LN<sub>2</sub>-cooled Ti:sapphire laser system delivers  $\leq 2.8$  mJ pulses at a rate of 1 kHz (alternatively  $\leq 1.8$  mJ at 2 kHz) with a pulse duration  $\geq 30$  fs (fwhm). Commissioning started in April 2004, observing THz radiation at the laser repetition rate in a newly constructed far-IR beamline. Since July 2004, laser-induced radiation is detected in the x-ray beamline with a signal-to-background ratio exceeding 10:1.

**Swiss Light Source:** The SLS femtoslicing project was initiated in 2001 [32]. Sufficient energy modulation at a beam energy of 2.4 GeV requires 5 mJ laser pulses, deliv-

ered at a rate of 1 kHz with 50 fs duration (fwhm) by a two-stage Ti:sapphire system, commissioned in 2004/5. Modulator and radiator will be placed in one 11 m long straight section with an s-shaped chicane between them for angular separation. Additional quadrupoles and the radiator, an in-vacuum undulator with 19 mm period length and 5 mm gap to produce 3-8 keV x-rays, were installed in 2004. The modulator with  $\lambda_U = 135$  mm and the bend magnets will be added in fall 2005.

**SOLEIL:** A feasibility study for femtoslicing at SOLEIL, a 2.75-GeV SR source under construction in Gif-sur-Yvette, was presented in 2004 [33]. Using a modulator ( $\lambda_U = 130$  mm and  $N_U = 20$ ) placed in a region with horizontal dispersion, energy-modulated electrons perform betatron oscillations and their radiation can be extracted at two different straight sections, proposing a helical undulator for 200-1000 eV photons and an in-vacuum undulator for x-rays up to 30 keV. A laser system with a pulse energy of 5-10 mJ with multi-keV repetition rate is envisaged.

## EXPERIMENTAL RESULTS

Successful laser-induced energy modulation can be detected and characterized by its effect on the laser spectrum, on the electron distribution and by the x-ray output.

### Effect on the Laser Pulse

Deviating from the resonance condition given by Eq. (1) causes a net energy transfer from the electrons to the laser field or vice versa, corresponding to a single-pass FEL or inverse FEL. At the ALS, the laser-electron interaction was demonstrated by measuring the difference of the light intensity above and below the central laser wavelength as function of the modulator gap [13, 21, 34].

### Effects on the Electron Distribution

**Longitudinal effects:** As electrons propagate through the magnetic lattice, the path length depends on the electron energy, horizontal position and angle. For laser-induced energy modulation, path length differences below  $\lambda_L$  cause a density modulation with a periodicity of the laser wavelength (micro-bunching), that can be used to generate coherent radiation at higher harmonics of  $\lambda_L$ . On the other hand, path length differences exceeding the laser pulse

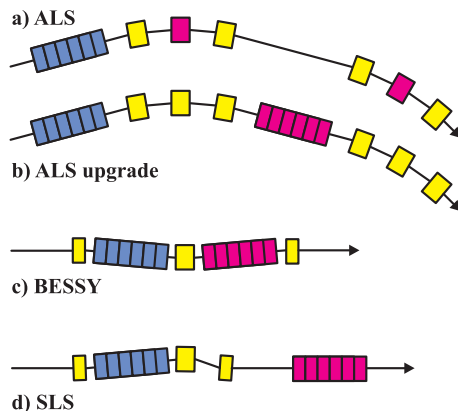


Figure 3: Footprints of femtoslicing facilities (not to scale) indicating the respective modulator (blue), the radiators (magenta) and bend magnets (yellow).

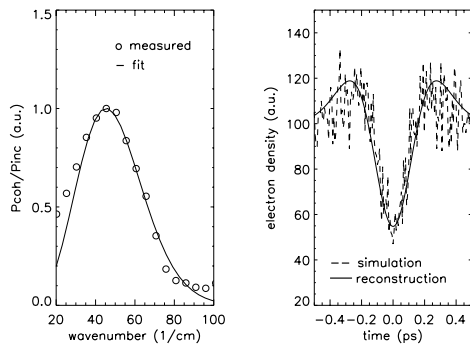


Figure 4: Left – ratio of coherent and incoherent THz radiation versus wavenumber. Right – the longitudinal electron distribution as reconstructed from the spectrum is consistent with simulation results [37].

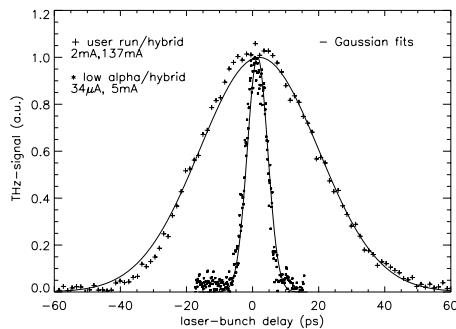


Figure 5: The THz signal from electron bunches in normal operation with reduced momentum-compactness factor ("alpha") as function of the laser pulse delay demonstrates the capabilities of femtoslicing as a diagnostics tool [37].

length create a dip and two side bumps in the longitudinal bunch profile, giving rise to coherent radiation in the THz regime. Observation of this radiation has become the prime diagnostics tool to monitor femtoslicing at the ALS [35] and at BESSY [36], where a dedicated THz beamline was constructed. Examples of THz data are given in Figs. 4 and 5 [37]. At the SLS, a dedicated THz beamline is planned as well [15].

**Transverse effects:** Without dispersion at the modulator, energy-modulated electrons will follow a dispersion orbit. Energy modulation in a dispersive region excites a betatron oscillation about the dispersion orbit, seen as a halo in pinhole images of the beam [25]. The transverse electron distribution directly reflects the energy modulation profile and can be probed quantitatively using a scraper while observing changes of the beam lifetime (see Fig. 6).

### Short-Pulse Synchrotron Radiation

At the ALS, visible light from the bend magnet radiator was cross-correlated with laser pulses to measure the time structure of transversely displaced energy-modulated electrons and the dark pulse at the bunch center [13, 21].

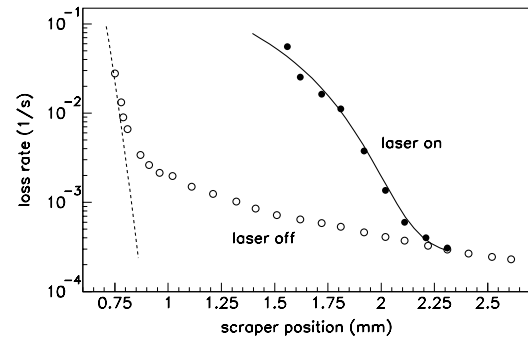


Figure 6: Loss rate versus scraper position with and without laser-induced energy modulation, where the dashed line indicates the quantum lifetime limit and the solid line is a simulation result [25].

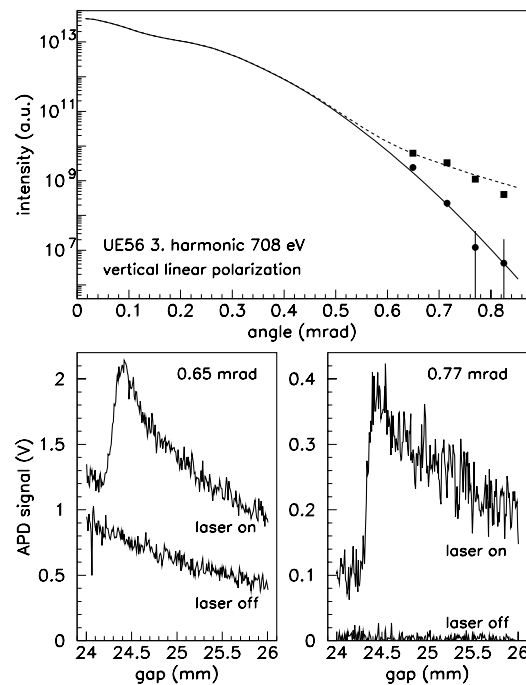


Figure 7: Top – calculated [38] and measured angular distribution of 708 eV radiation with and without laser-induced energy modulation. Bottom – 3rd harmonic of the UE56 radiator for two observation angles [27].

With the BESSY separation scheme, laser-induced x-rays are readily detectable in the angular distribution of monochromatized radiation at the x-ray beamline, using an avalanche photodiode (Fig. 7, top). Moving the UE56 radiator gap while keeping the monochromator fixed scans the 3rd undulator harmonic (Fig 7, bottom). A fraction of the short-pulse radiation has a flat spectral distribution, caused by off-angle photons (relative to their respective source electron). This background is of particular relevance for the generation of short x-ray pulses with circular polarization, since off-angle photons may have the wrong helicity and would reduce the net polarization.

## CONCLUSIONS AND OUTLOOK

It is expected that three femtoslicing facilities will produce sub-picosecond undulator radiation by the end of 2005: at BESSY, the ALS and the SLS.

Femtoslicing shares the advantage of tunability in energy and polarization with conventional SR. An obvious drawback is the low photon flux, limited mainly by the laser repetition rate, but the flux per bandwidth is still superior to that of laser-based HHG sources [5] above a photon energy of 200 eV. Plasma sources at multi-keV energies, on the other hand, lack the tunability of SR and are fully divergent.

Compared to other schemes based on storage rings, the advantages of femtoslicing are the potential of generating sub-100 fs x-rays and their natural synchronization to laser pulses for pump-probe applications. In "low- $\alpha$ " operation of BESSY ( $\alpha$  denoting the momentum-compactness factor), the rms pulse duration has fallen below 1 ps [8], but its continuation to the 100-fs level at the expense of bunch current would yield a photon flux similar to that of femtoslicing. While low- $\alpha$  and rf deflection schemes can be applied at the maximum bunch rate, the repetition rate in pump-probe experiments is limited by the lower of the two pulse rates, and the full bunch frequency might not be usable.

Linac-driven FELs [11, 12] are expected to be the ultimate short-pulse sources, delivering femtosecond (or even attosecond) x-ray pulses with high brightness. In this context, femtoslicing is not a competitor but a unique opportunity to practise laser-induced energy modulation as a basis for FEL seeding and attosecond-pulse generation schemes and to test novel short-pulse synchronization and detection techniques.

Finally, it might be possible to take the femtoslicing technique one step further by energy-modulating electrons using amplified few-cycle laser pulses with stabilized carrier-envelope phase [39] to generate attosecond pulses. Here, the challenges are isochronicity and stringent background elimination. Yet another potential of femtoslicing is the generation of shape-controlled x-ray pulses. The pulse shaping technique, that has become fashionable with laser pulses to control e.g. chemical reactions [40], is not directly applicable to SR, lacking sufficient coherence. However, femtoslicing can leave an imprint of a shape-controlled laser pulse on the electron bunch to produce the desired x-ray pulse shape.

## ACKNOWLEDGEMENTS

Valuable contributions to this paper were received from A. Cavalleri, R. Schoenlein, A. Zholents (LBNL, Berkeley), P. Beaud, G. Ingold (SLS, Villigen) and A. Nadji (SOLEIL, Gif-sur-Yvette). As for the BESSY facility, I am very much indebted to all colleagues contributing to the project, and in particular to those who shared all the night shifts: K. Holldack, T. Kachel, R. Mitzner and T. Quast.

## REFERENCES

- [1] D. Attwood, *Soft X-Ray and Extreme Ultraviolet Radiation*, Cambridge University Press (1999).
- [2] J. Als-Neilsen, D. McMorrow, *Elements of Modern X-Ray Physics*, John Wiley & Sons (2001).
- [3] D. Strickland, G. Mourou, *Opt. Commun.* 55 (1985), 447.
- [4] A. M. Lindenberg et al., *PRL* 84 (2000), 111.
- [5] E. Seres, J. Seres, F. Krausz, C. Spielmann, *PRL* 92 (2004), 163002.
- [6] C. Rischel et al., *Nature* 390 (1997), 490.
- [7] K.-J. Kim, S. Chattopadhyay, C. V. Shank, *NIM A* 341 (1994), 351.
- [8] J. Feikes, K. Holldack, P. Kuske, G. Wüstefeld, EPAC'04, Lucerne (2004), 1954.
- [9] A. A. Zholents, M. S. Zoloterev, *PRL* 76 (1996), 912.
- [10] A. Zholents, P. Heimann, M. Zoloterev, J. Byrd, *NIM A* 425 (1999), 385.
- [11] B. Faatz, this conference (PAC'05), TOAB002.
- [12] D. Krämer, this conference (PAC'05), RPPT001.
- [13] R. W. Schoenlein et al., *Science* 287 (2000), 2237.
- [14] S. Khan et al., EPAC'04, Lucerne (2004), 2287.
- [15] G. Ingold et al., PSI Scientific Report 2002-2004, Vol. III, and priv. communication.
- [16] L. H. Yu, *Phys. Rev. A* 44 (1991), 5178.
- [17] A. A. Zholents, PRST-AB 9 (2005), 040701.
- [18] E. L. Saldin, E. A. Schneidmiller, M. V. Yurkov, *Opt. Commun.* 237 (2004), 153.
- [19] E. L. Saldin, E. A. Schneidmiller, M. V. Yurkov, *Opt. Commun.* 239 (2004), 161.
- [20] A. A. Zholents, W. M. Fawley, *PRL* 92 (2004), 224801.
- [21] R. W. Schoenlein et al., *Appl. Phys. B* 71 (2000), 1.
- [22] A. Zholents, W. Decking, EPAC'00, Vienna (2000), 723.
- [23] Spectral separation was proposed by H. Padmore, LBNL.
- [24] A. Amir and Y. Greenzweig, *Phys. Rev. A* 34 (1986), 4809.
- [25] K. Holldack, T. Kachel, S. Khan, R. Mitzner, T. Quast, PRST-AB 8 (2005), 040704.
- [26] S. Khan, this conference (PAC'05), RPAE034.
- [27] S. Khan, K. Holldack, T. Kachel, R. Mitzner, T. Quast, this conference (PAC'05), RPAE033.
- [28] A. Cavalleri et al., LBNL, preprint cond-mat/0503311.
- [29] R. Schoenlein, priv. communication (2005).
- [30] C. Steier et al., PAC'03, Portland (2003), 397.
- [31] S. Khan et al., PAC'03, Portland (2003), 836.
- [32] G. Ingold et al., PAC'01, Chicago (2001), 2656.
- [33] A. Nadji et al., EPAC'04, Lucerne (2004), 2332.
- [34] R. Schoenlein et al., PAC'99, New York (1999), 2498.
- [35] J. Byrd et al., EPAC'04, Lucerne (2004), 2448.
- [36] K. Holldack et al., EPAC'04, Lucerne (2004), 2284.
- [37] K. Holldack et al., this conference (PAC'05), RPAE032.
- [38] Using the code WAVE, M. Scheer, BESSY (unpublished).
- [39] A. Baltuška et al., *IEEE J. Quant. Electron.* 9 (2003), 972.
- [40] R. S. Judson and H. Rabitz, *PRL* 68 (1992), 1500.